coatings

MDPI

Article

Evaluation of Curing Effects on Bitumen Emulsion-Based Cold In-Place Recycling Mixture Considering Field-Water Evaporation and Heat-Transfer Conditions

Zili Zhao [1], Fujian Ni [1,*], Junqiu Zheng [2], Zhiqiang Cheng [3,4,*] and Shengjia Xie [3,4]

[1] College of Transportation Engineering, Southeast University, Nanjing 211189, China; zili_zhao@seu.edu.cn
[2] Engineering & Technology Department, Jiangsu Communications Holding Co., Ltd., Nanjing 210002, China; zjq20140811@sina.com
[3] Shanghai Road and Bridge Group Co., Ltd., Shanghai 200433, China
[4] Shanghai Engineering Research Center of Green Pavement Materials, Shanghai 200433, China
* Correspondence: 101004746@seu.edu.cn (F.N.); cr1903@tongji.edu.cn (Z.C.)

Abstract: The strength growth of a bitumen emulsion-based cold in-place recycling asphalt mixture (BE-CIR) is time-dependent and time-consuming due to the addition of water. There is a great difference between the curing conditions of specification in the laboratory and the in situ conditions, which often leads to a great discrepancy between the results of lab specimens and the field cores. The main objective of this paper is to evaluate the curing effect on laboratory BE-CIR considering field-water evaporation and heat-transfer conditions. Four different curing methods were designed by using different combinations of waterproof layers, heat insulation layers, and variable temperature modes. The variations in temperature indexes, moisture content, air void, and indirect tensile strength (ITS) with curing time were tested, and the mutual influence of these indicators was analyzed. Furthermore, the results of the laboratory samples were compared with the field cores. Testing results show that the performance of the BE-CIR mixture is significantly different from that with no treatment, which is manifested as higher moisture content and lower air void and ITS under the same curing time. The internal temperature of the mixture is the main factor affecting the variation of moisture content, especially on the first curing day. The air void of the mixture has a strong linear relationship with the moisture content. Moisture content and ITS under different curing methods showed similar trends and could be divided into two stages. Taking the field cores as a benchmark, it can be concluded that the field-water evaporation condition should be considered in the setting of indoor curing methods, while the heat transfer could not.

Keywords: bitumen emulsion; cold in-place recycling; curing method; indirect tensile strength; field cores

Citation: Zhao, Z.; Ni, F.; Zheng, J.; Cheng, Z.; Xie, S. Evaluation of Curing Effects on Bitumen Emulsion-Based Cold In-Place Recycling Mixture Considering Field-Water Evaporation and Heat-Transfer Conditions. *Coatings* **2023**, *13*, 1204. https://doi.org/10.3390/coatings13071204

Academic Editor: Enrico Quagliarini

Received: 7 June 2023
Revised: 2 July 2023
Accepted: 4 July 2023
Published: 5 July 2023

1. Introduction

Bitumen Emulsion-based Cold In-place Recycling (BE-CIR) is an environmentally friendly pavement maintenance technology that allows a high percentage of reuse of reclaimed asphalt pavement (RAP), eliminating the requirement for heating and transport during recycling [1–3]. In recent years, it has garnered global recognition and adoption in many countries due to its cost-effectiveness and environmental sustainability [4,5]. It also boasts a range of appealing attributes, including the capability to comprehensively address pavement distresses such as potholes, rutting, irregular cracks, and reflection cracks, and also has the potential to significantly prolong the service life of asphalt pavement, alleviate the burden of landfill disposal, and enhance the overall riding comfort [6–8]. To improve the early strength of BE-CIR mixtures, additives such as cement, fly ash, and lime are often added to the BE-CIR mixture. These additives can facilitate the accelerated breaking of the bitumen emulsion and promote strong bonding between the RAP aggregate and mortar through hydration reactions [9–11].

In contrast to conventional hot-mix asphalt (HMA), the BE-CIR mixture requires the addition of extra water to meet the workability criteria during compaction, ensure a sufficient coating of the bitumen emulsion, and achieve maximum density by lubricating the mixture [12–14]. Due to the presence of moisture and a cementitious co-binder, the evaluation of the performance development of the BE-CIR mixture necessitates taking into account the curing time. Research has revealed that in the early stage of curing time, cement has an important influence on the early strength growth rate of the BE-CIR mixture, while bitumen emulsion plays a decisive role in the initial value of strength and the final in-service strength [15]. During the curing process, a small proportion of water combines with the active minerals (e.g., cement) to form hydration products, while the majority of the free water leaves the system through evaporation [16,17]. This process is greatly affected by external conditions, including temperature, humidity, etc. [18–20], so that the performance of BE-CIR mixtures has significant time-varying characteristics. Because of this, in practical BE-CIR technology projects, it generally needs curing for few days before the construction of the upper structure can continue. This requirement limits the application scope of the technology to a certain extent. Therefore, it is of great significance to study the time-varying performance of BE-CIR mixtures during the curing period to increase the application scenarios of this economically and environmentally beneficial technology.

In order to study the performance change of BE-CIR mixtures in the laboratory, the premise is to simulate the in situ conditions in a laboratory setup. Several curing methods have been compared to obtain the development of strength formation and moisture loss during curing of BE-CIR, such as specimens covered with an impervious material or sealed and cured in a plastic bag [21–23]. Meanwhile, researchers have adopted a combination of varying times, temperatures, and humidity levels to simulate environmental curing conditions [24–26]. However, the aim of most of the current recommended laboratory-curing conditions is to accelerate the actual field-curing process. For example, BE-CIR specimens were recommended to cure in a temperature-controlled oven at 60 °C for 2 days after fabrication [27]. Whereas this may be beneficial for evaluating the structural contribution of the BE-CIR mixture when it is fully cured, it may not be capable of providing conditions to study time-varying characteristics of mixtures. Additionally, the use of high temperatures to accelerate the curing process may change the properties of the mixture.

However, under field-curing conditions, the internal temperature of the pavement is constantly fluctuating due to ambient temperature [28,29], and only the upper surface is in contact with the external environment until the cover layer is constructed. Since few studies have considered the moisture and heat conditions, like field, in laboratory simulations, results of the mechanical performance's development during curing could hardly correspond to the field-cored samples. To fill this gap, this study aims to establish a practical laboratory-curing method simulating in situ curing conditions as much as possible. The main objectives of this research are: (1) investigate the properties, including temperature indexes, volume parameters, moisture content, and indirect tensile strength (ITS), during the curing time considering field-water evaporation and heat-transfer conditions; (2) explore the mutual influence between properties during the curing process; (3) evaluate the designed curing method based on the results of the field-core samples.

2. Materials and Experimental Program

2.1. Mix Design

This work was based on a highway maintenance project using BE-CIR technology in Lianyungang, China. The structure design for this project was to regenerate the original 10 cm surface layer into an entire BE-CIR layer, followed by a 5 cm overlay layer on top of it. The materials and mixture design were consistent with the project [30]. Therefore, the laboratory samples were prepared using pure RAP, and the gradation of RAP material from this project fell within the medium gradation limitations specified by the Jiangsu Province agency [31], as demonstrated by the black curve in Figure 1. One cationic slow-setting

emulsified bitumen was used and its basic properties are listed in Table 1 based on Chinese standards [32].

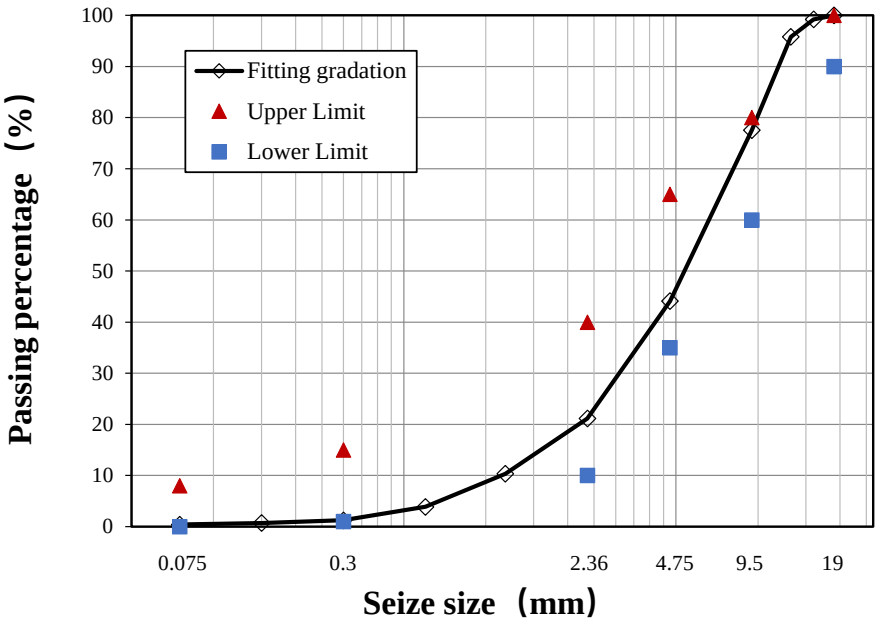

Figure 1. Aggregate gradation of CIR mixtures.

Table 1. Properties of emulsified bitumen.

Characteristics of the Emulsified Bitumen	Result
Residual content (%)	64
Penetration (25 °C; 0.1 mm)	59.1
Softening point (°C)	59.9
Ductility (15 °C; cm)	110
Sieve residue (1.18 mm; %)	0.03
Storage stability (5 d, 25 °C; %)	1.47
Storage stability (1 d, 25 °C; %)	0.42

An ordinary Portland cement (PO. 42.5) from Anhui Conch Cement Co., Ltd, (Hong Kong, China) was selected as an additive in this project. It is important to highlight that since the BE-CIR mixture in this project was used in the asphalt layer, and the CIR layer was only topped by a 5 cm overlay. In order to solve the problems of the lack of high-temperature performance and the weak early strength, a relatively higher cement content of 2.2% was determined based on previous project experiences. The optimum emulsified bitumen content was determined to be 3.3% by weight of the RAP based on the results from Marshall Stability and Indirect Tensile Strength. The optimal moisture content was obtained using the maximum dry density method as 4.01% by weight of the RAP [33]. The composition of the optimum moisture content included the water in the emulsified bitumen as well as the extra water. Since the residue content by evaporation of emulsified bitumen was 64%, the water in the emulsified bitumen was 1.188% (3.3 × 0.36), and the content of extra water was therefore calculated to be 2.8%. Table 2 shows the mixture design parameters based on the Jiangsu Province agency [31]. In this process, the specimens were compacted using a Marshall hammer with 75 blows per side, then cured in a temperature-controlled oven at 60 °C for 48 h and finally cooled at room temperature for 12 h for subsequent tests.

Table 2. Properties of mixture design.

Properties of Mixture Design	Results
Optimal emulsified bitumen content (%)	3.3
Cement content (%)	2.2
Optimal moisture content (%)	4.01
Bulk density (g/cm^3)	2.184
Target air voids (%)	10.0

2.2. Curing Method Design

In most of the field projects in China, there are usually several days of curing depending on the external environment for the BE-CIR layer before the construction of the cover layer. It is difficult to determine the exact curing time required in the actual field condition using the methods in the specification. Therefore, in an attempt to provide a better approach to solving this problem, this paper only considers the development of the mixture properties during curing prior to overlay. Based on this, compared with the actual project condition, two main aspects of water evaporation and heat transfer are not considered in curing conditions of the current specification. In order to solve these two problems, two targeted specimen preparation methods are proposed in this paper. The first is to simulate the actual moisture evaporation by adding a waterproof layer to the specimen. As shown in Figure 2a, after the mixture is fabricated, a fully enclosed tarpaulin is wrapped around its sides and bottom surface. This method leaves only the upper surface of the mixture in contact with the external environment, so that moisture inside the mixture can only evaporate from the upper surface. The second is to simulate the heat transfer by applying an insulation treatment to the specimens, as shown in Figure 2b. A thermal insulation pad is wrapped around the specimen, which leads to heat transfer from the upper surface only. One important assumption of this simulating method in this paper was ignoring the effect of the material on the moisture migration in the substructure of BE-CIR layer as well as on the sides. In the project for this paper, the substructure was a densely graded asphalt layer with almost zero percolation rate whose impact could be neglected, while for other different substructures this method could be improved.

(**a**) (**b**)

Figure 2. Simulation of curing schematic (**a**) waterproofing (**b**) heat insulation.

For the temperature conditions during the curing period, two different temperature control modes are considered. One is constant temperature mode, which means during the curing time, the temperature remains the same, and this mode is similar to the specification. Another is variable temperature mode, which is formed by a programmable environmental

chamber to achieve temperature conditions close to those in the field. The settings of the curing temperature were mainly based on the BE-CIR project of Fenguan highway (G15) in June 2021. Based on the results of the temperature measurement of the road surface on site, it is known that the temperature of the road surface can reach 50 °C at the highest temperature at noon and drop to around 20 °C at the lowest temperature at night. More details on field temperature can be found in our previous study [30]. Therefore, for constant temperature mode, the constant temperature was set to the highest and lowest average temperature of 35 °C. For variable temperature mode, due to the difficulty of simulating the real temperature change of each day, a segmented temperature control method was applied in this study. Since the temperature of road surface is influenced by the solar radiation, according to the observation in the field, road surface temperature is relatively high during 8:00–18:00 each day. Therefore, for variable temperature mode, 10 h high temperature +14 h low temperature was set. In order to be closer to the actual project, 45 °C was used for high temperature and 25 °C was used for low temperature. The relative humidity during curing was set as 45% controlled by the environmental chamber.

Combining different specimen-preparation methods and temperature-control modes, four different curing methods are designed in this paper. As shown in Table 3, for the convenience of expression, "N", "W", and "WT" represent different specimen-preparation methods, namely no treatment, waterproofing, and waterproofing + heat insulation, respectively. "C" and "V" stand for constant temperature mode and variable temperature mode, respectively.

Table 3. Design of curing methods.

Curing Method	Specimen-Preparation Method	Temperature-Control Mode
N + C	No Treatment	Constant 35 °C
W + C	Waterproofing	Constant 35 °C
W + V	Waterproofing	Variable 10 h (45 °C) + 14 h (25 °C)
WT + V	Waterproofing + Heat Insulation	Variable 10 h (45 °C) + 14 h (25 °C)

2.3. Test Program

Previous studies have shown that the Superpave gyratory compaction method is more in line with the actual situation of pavement construction than the Marshall compaction method. Therefore, the Superpave gyratory compaction method was chosen to prepare BE-CIR mixture in this paper. In order to match the actual project, specimens with a diameter of 100 mm and a height of 100 mm were compacted. The gyratory count was set to 30 to achieve the same air void as the in situ project. All specimens were compacted by the same number of gyrations using the same mass.

Since one of the significant objectives of this study was to observe the performance development of a cold recycled mixture during the curing period under different curing conditions, five different curing days, namely 1, 3, 7, 14, and 28 d, were selected. Three replicate specimens were compacted for each day, so that fifteen replicate specimens were prepared for each curing condition. Considering four different conditions, a total of 60 specimens were produced; part of them are shown in Figure 3a. Two programmable environmental chambers were applied for different temperature-control modes. In addition, temperature sensors were buried in the specimens to obtain the temperature variation inside the mixture under different curing conditions. Considering the N + C method has no preparation treatment with the constant permaculture temperature, the internal temperature of the mix would keep consistent with the environmental temperature. Therefore, a sample was selected from each of the other three curing methods to monitor internal temperature changes, considering that if the temperature sensor was installed in the core of specimens, the installation process would inevitably cause an eventual damage and mass loss. The temperature sensors were stuck to the sample surface before the waterproofing, so the measured temperature was only the surface temperature of the specimen, which

may be slightly different from that inside the sample. This can be seen in Figure 3b; two temperature sensors were installed at 25 mm and 75 mm from top to bottom, respectively.

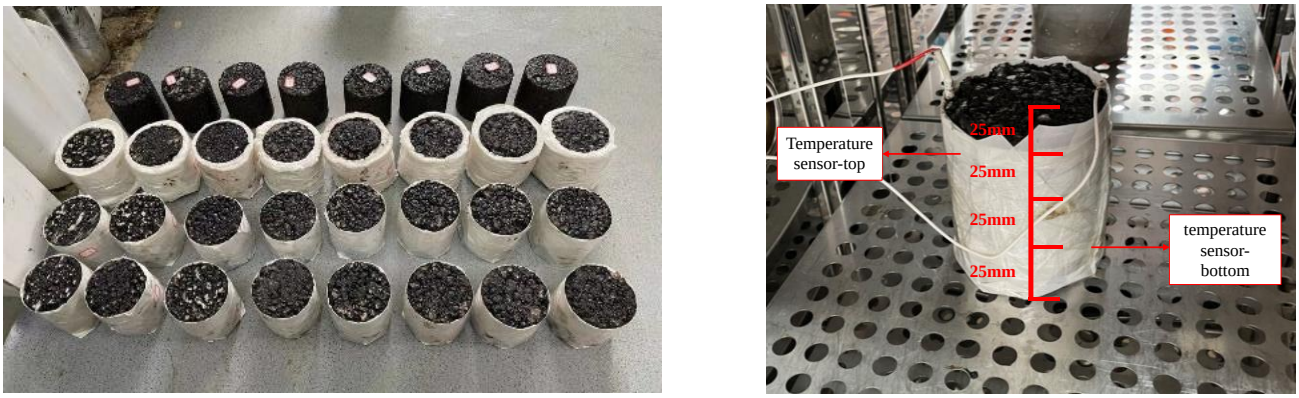

(**a**) Specimen for different curing method (**b**) Sensor embedment

Figure 3. Specimens preparing and testing.

In this study, several material properties, including the water loss, moisture content, bulk volume relative density (γ_f), air void (AV), and indirect tensile strength (ITS) of BE-CIR mixture during curing period, were tested. The daily mass of each sample was recorded to calculate the water loss. The moisture content of each sample was also calculated based on the water content in the initial state. After curing 1, 3, 7, 14, and 28 days, three replicate specimens of each curing method were taken out. The bulk volume relative density (γ_f) of each specimen was tested and the air void (AV) could be therefore calculated according to AASHTO T 269 [34]. The ITS carried out at 15 °C was measured after testing γ_f. Before ITS tests, the upper part of the specimen with a height of 63.5 cm (measured down from the side in contact with the environment) was cut out for testing due to the dimensional requirements of the indirect tensile strength test. In addition, field-cored samples with a diameter of 100 mm were collected from this project at different times of curing to test ITS the same as laboratory specimens.

3. Results Analysis

3.1. Analysis of Temperature Variation

To evaluate the temperature variation of specimens under different curing methods, one temperature cycle (24 h) was selected for analysis, as shown in Figure 4. It was found that there was a great difference in the temperature variation between different curing methods. For the method W + C, the specimen rose rapidly to the set temperature and then remained stable. However, the two curing methods with variable temperature modes had two phases in each cycle. Specimens from the W + V method were similar to those from the W + C, rising rapidly to the maximum temperature of 45 °C and falling rapidly to 25 °C when cooling down. Because of the presence of insulation, the internal temperature of the WT + C method both rose and fell more slowly. The maximum temperature of WT + C did not reach the environmental temperature of 45 °C and the minimum temperature was also slightly less than 25 °C. Comparing results in the two different positions at the top and bottom, the results under different curing methods were similar, which means temperature in the top part is higher than that at the bottom part in the high-temperature phase, while lower in the low-temperature phase. This is mainly due to the high heat capacity and low thermal conductivity of BE-CIR, which leads to a slower temperature change inside than on the surface, and the phenomenon is also consistent with the data measured in the field [30].

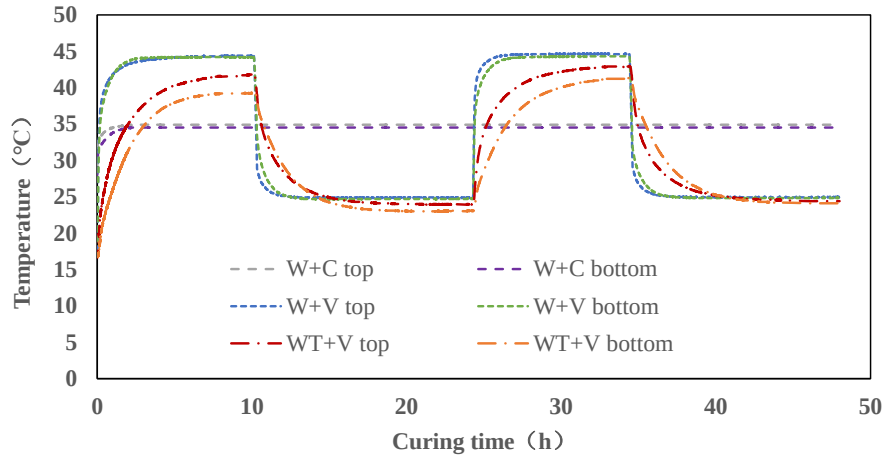

Figure 4. Temperature change curve for different curing methods.

In order to quantitatively analyze the curve of temperature-curing time, some indices were extracted from the curve, as shown in Figure 5. Firstly, the temperature-curing time curve of one cycle was divided into two phases—the high-temperature phase and the low-temperature phase. Each phase had three indexes, including maximum or minimum temperature, heating or cooling time, and Gt. The maximum and minimum temperatures were recorded as T-max and T-min, respectively. The time required to reach the maximum or minimum temperature was defined as the heating time or cooling time. The area enclosed by the time-temperature curve was defined as Gt, which can be interpreted as the temperature energy. It can be inferred that higher Gt indicates the specimens that absorbed or dissipated more heat at this stage. The Gt for the high and low-temperature phases was denoted as Gt-h and Gt-l, respectively. Two indicators were chosen for the whole cycle, the average temperature (T-a) and the total Gt (Gt-a). The results of these indicators are shown in Table 4.

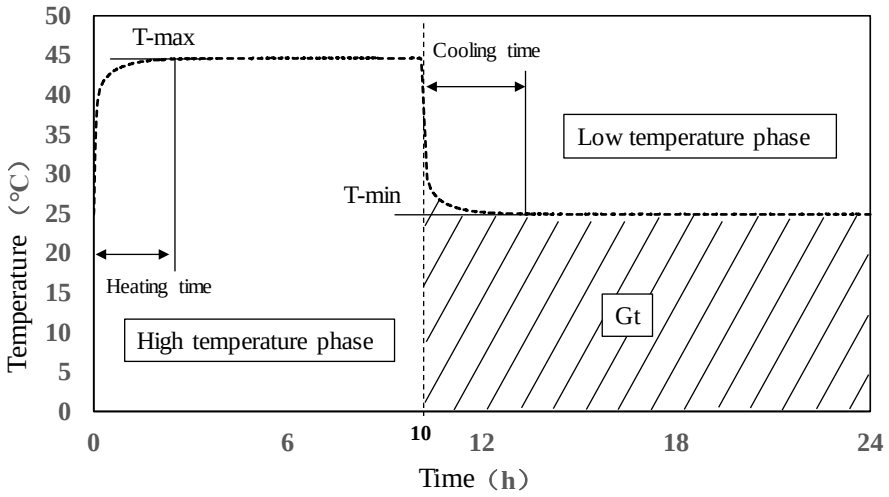

Figure 5. Quantitative analysis of temperature-curing time curve.

From Table 4, considering the full cycle, the T-a and Gt-a of W + C were the largest of the four curing methods, and the T-a was close to the set temperature of 35 °C. However, the T-a and Gt-a of the another two variable temperature modes had great differences. The T-a of WT + V was larger than that of W + V, while the Gt-a of WT + V was smaller. This is mainly due to the fact that the curve for WT + V rose and fell more slowly, which led to a concentration of temperature, resulting in a larger T-a. W + V remained at its T-max for a longer time, resulting in a larger Gt-a under the whole cycle. Comparing different

positions of the mixture, both T-a and Gt-a were greater at the top than the bottom of the different methods.

Table 4. Quantitative analysis index of temperature for different curing methods.

Property	W + C-Top	W + C-Bottom	W + V-Top	W + V-Bottom	WT + V-Top	WT + V-Bottom
			High-temperature phase (0–10 h)			
T-max (°C)	34.9	34.5	44.7	44.6	43	41.3
Heating time (h)	2	2.1	2.5	3.3	7.9	8.5
Gt-h (°C·h)	348.07	343.28	442.88	436.95	405.44	377.50
			Low-temperature phase (11–24 h)			
T-min (°C)	34.9	34.5	24.9	24.8	24.4	24.1
Cooling time (h)	-	-	3.2	3.9	10.6	11
Gt-l (°C·h)	488.21	482.62	355.29	356.20	368.13	374.01
			Full cycle			
T-a (°C)	34.84	34.41	32.86	32.65	33.35	32.34
Gt-a (°C·h)	836.28	825.90	798.17	793.15	773.58	751.51

For different phases, in the high-temperature phase, the heating time of W + C method was only 2 h, and the three indexes of the upper and bottom were essentially the same. Specifically, the heating time of W + V was longer than that of W + C due to the difference in T-max. Meanwhile, the heating time for the top and bottom was also different, with the bottom being 3.3 h, 0.8 h longer than the 2.5 h in the top position. Additionally, the Gt-h at the top of W + V was the largest among the different methods. WT + V had a slightly lower T-max compared with W + V, and the top and bottom positions were 43 °C and 41.3 °C, respectively, which were 1.7 °C and 2.3 °C lower than the corresponding top and bottom position of W + V. In addition, the heating time of WT + V was considerably longer, with the top and bottom position being 7.9 h and 8.5 h, respectively, which lasted almost the entire high-temperature phase. Also, WT + V presented a smaller Gt-h compared with W + V; the order of Gt-h was W + V > WT + V > W + C. In the low-temperature phase, the cooling time of W + V was longer than the heating time, with the top and bottom parts being 3.2 h and 3.9 h, respectively, and the corresponding Gt-l was the smallest among the three methods. Similarly, comparing WT + V to W + V, WT + V showed slightly lower T-min, longer cooling time, and greater Gt-l. Therefore, the order of Gt-l became W + C > W + V > WT + V.

It can be concluded from the comparison that the average temperature of the variable temperature mode was lower than that of the constant temperature mode. When the insulation was added, the temperature change became slower. However, from the difference in heating and cooling time between the top and bottom position in W + C and W + V, it could also indicate that the waterproofing layer plays a certain role in blocking heat transfer. This may be also because of the fact that water in the specimens with waterproofing only diffuses in one direction, resulting in a difference in water content in thickness direction, which also affects the temperature transmission.

3.2. Moisture Variation Analysis

The results of moisture content over curing time are shown in Figure 6. The initial value for moisture content was 4%. It can be seen from the figure that under different curing methods, the water content decreased rapidly in the early stage, and remained stable as curing time increased. However, there are significant differences between the four curing methods. The moisture content of the N + C method was obviously lower than the other three methods, only 0.29% at twenty-eight days, and decreased rapidly in the first few days, especially from 4% to 1.547% on the first day. After curing for 7 days, the moisture content dropped to less than 1% and stayed stable earlier than the other methods, mainly because the water inside can diffuse freely from all sides of the specimen. For the other three curing methods, the curves of moisture content over curing time are relatively similar due to the

specimen preparation of the waterproofing. The moisture content was still more than 2% after 5 days of curing, and it tended to be stable in about 12 days. Between the three curing methods, the moisture content ranked W + C < W + V < WT + V from 0 to 10 days, while after 10 curing days the moisture content of W + V gradually converged with that of W + C. Eventually, the water content of W + V and W + C kept almost the same after curing for 28 days (0.974% and 0.943%, respectively), which were smaller than that of WT + V (1.18%), while obviously greater than N + C (0.29%), indicating that there was still a significant amount of residual water within the mixture and this water may continue to dissipate with increasing curing.

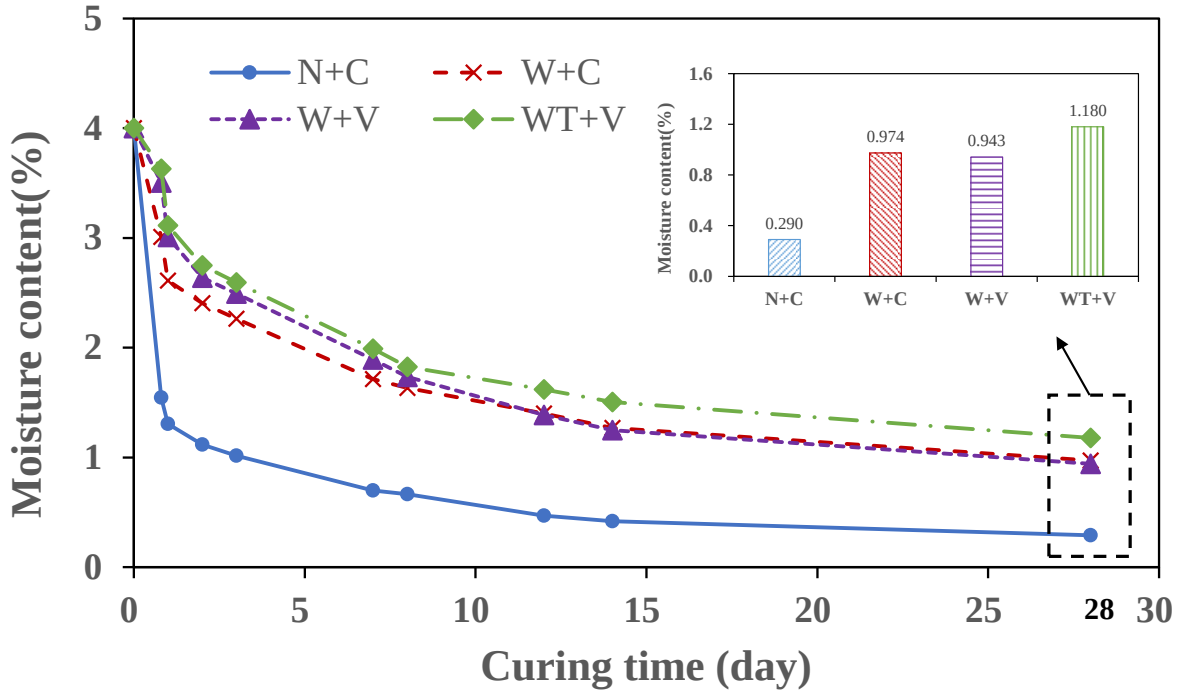

Figure 6. The variation of moisture content with curing time.

It is well-known that the changes in moisture content are mainly influenced by temperature, and the analysis of temperature shows that the rank of T-a is W + C > WT + V > W + V, while that for Gt-a is W + C > W + V > WT + V, indicating that Gt-a is consistent with the regularity exhibited by water content. Furthermore, considering the high- and low-temperature phases, Gt-h is W + V > WT + V in the high-temperature phase, while it is the opposite for Gt-l in the low-temperature phase, which infers that the high-temperature phase has a greater effect on the moisture content of the specimen.

3.3. Analysis of the Changing Air Void Content

In Figure 7, it can be found that the air void of the samples under different curing methods increases with the increase in curing time. This phenomenon is reasonable because after the BE-CIR mixture is formed, the internal voids are filled with free water. During the curing time, the free water in the voids is partially hydrated with the cement, and the rest of the water undergoes phase changes and evaporates into the environment, resulting in a continuous increase in the air void of the mixture. As can be seen from Figure 7, the air void for the N + C method is much greater than that for the other three methods and increases rapidly in the early stages, reaching 9.88% at 7 days, and remains essentially stable after curing for 7 days. The air void of the other three methods increases gradually with the curing time and does not reach a similar period of stability to N + C. The increase between 14 and 28 days is still 0.2%–0.3% for the three methods except N + C. Comparing those three curing methods, the air void of different methods did not show a consistent

regularity under different curing days, and remained essentially the same when curing time was longer than 14 days. However, it is theoretically clear that the variety in air void was mainly caused by the dissipation of internal moisture, since the rank of moisture content was W + C < W + V < WT + V, and specimens with lower moisture content should have a greater air void. It can also be found that the variability in air voids is relatively large, and the maximum difference between different samples can reach 0.5%. When compared with N + C, the air void is well-discriminated due to differences between 0.8% and 1.6%, while comparisons between W + C, W + V, and WT + V show only 0.1%–0.3% differences in air voids between them, and this difference is even smaller than the variability in the test methods.

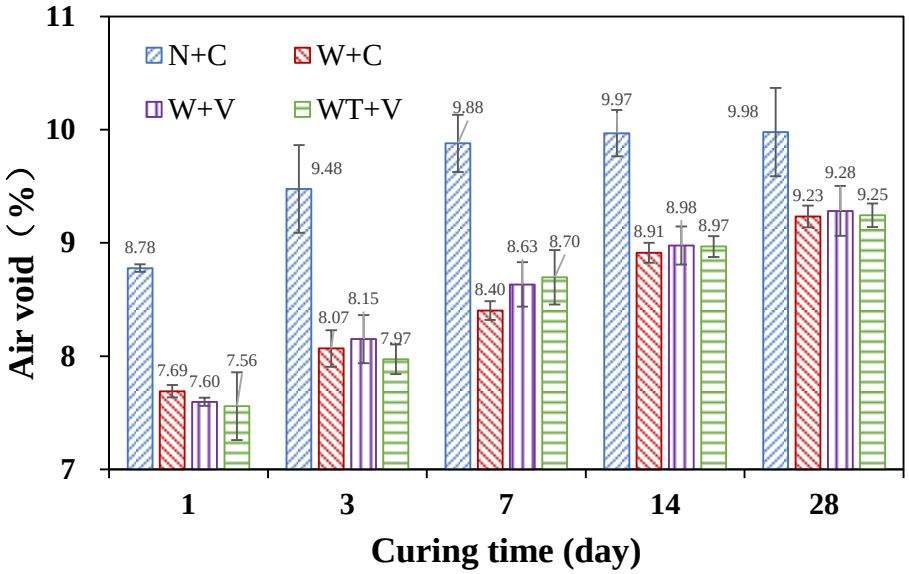

Figure 7. Variation in air void with curing time.

3.4. Analysis of the ITS

The variation in ITS with curing time for the different curing methods is shown in Figure 8. ITS increased over curing time but showed great differences between curing methods. Similar to moisture content and air void, the ITS of N + C was significantly greater than that of the other three curing methods since the optimum water content for cement was about 1/3 of its mass, i.e., about 0.8% water (as opposed to 2.2% cement). However, during the curing process, according to the results in Section 3.2, the moisture content of N + C was about 1% after 3 days of curing, whereas the other three methods were all greater than 2%, which was greater than the optimum water content for cement. The higher water content may, thus, inhibit the hydration of the cement, contributing to the lower ITS of the BE-CIR. In addition, the ITS of N + C increased from 0.74 MPa (14 d) to 0.963 MPa (28 d) due to continuous hydration of the cement, which is close to the increase from days 1 to 14 (0.253 MPa).

The other three curing methods had relatively low ITSs of less than 0.28 MPa on day 1, with 0.2 MPa smaller than N + C. From day 1 to day 3, the ITS increased rapidly, and the gap between N + C was only less than 0.12 MPa after curing for 14 days. The rank of these three methods was W + C > W + V > WT + V, which was consistent with the rank of moisture content, suggesting that higher moisture content inhibits cement hydration even more. Moreover, it could be found that there was great difference for the three curing methods with N + C at 28 days, similar to moisture content and air void, indicating that the curing may be still in progress after curing for 28 days at least for the sealed specimens. This is mainly due to the fact that the cement is not fully hydrated in this condition because of the high moisture content. It is interesting whether or when these indexes converge with

different curing methods and different curing conditions; more studies will be conducted in the future.

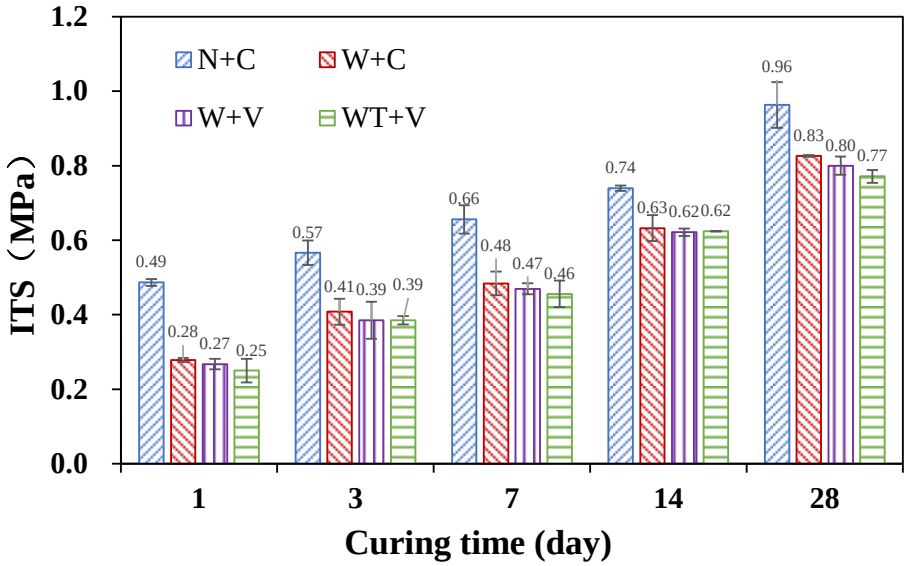

Figure 8. Results of ITS over curing time.

4. Mutual Influence of Indicators

In Section 3, four indicators of temperature, moisture content, air void, and ITS were analyzed over curing time, and clearly there was a strong connection between these four indicators. Theoretically, the temperature changes inside specimens under different curing methods directly affect the moisture content, and since free water mainly exists in the voids, the decrease in water content will directly cause the change in the air void. The ITS of the mixture is the result of the comprehensive influence of the curing conditions. Therefore, this section's analysis of the mutual influence of different indicators includes temperature indexes with moisture content, moisture content with air void, and moisture content/air void with ITS. The average value of these indicators was used in this section.

4.1. Effect of Temperature Indexes on Moisture Content

Since specimens of the N + C method were not treated with a waterproofing layer, although it had the same temperature conditions as the W + C method, the moisture content decreased faster due to how it could be dissipated from all sides of the specimens. It proved that the waterproofing layer had a significant effect on changes in the moisture content of the specimen. Therefore, results of the other three curing methods were detailed and analyzed.

From Section 3.2, the moisture content of different curing methods displays as W + C < W + V < WT + V, which corresponds to the rank of Gt-a. Figure 9a illustrates the moisture content and Gt-a. The rank of Gt-a was always W + C > W + V > WT + V since Gt-a is accumulated continuously with curing time. However, the rank of moisture content was different. During the first 7 curing days, the moisture content of W + C was the smallest and that of WT + V was the largest. When the curing period exceeded 14 days, the moisture content of W + C and W + V were closer, while that for WT + V was still the largest, which exhibited that for the specimens with only the treatment of waterproofing, the effect of different temperature modes on the moisture content decreased with time, and there was almost no effect after curing for 14 days. In addition, from the comparison of the W + V and WT + V methods, it can be seen that the influence of the thermal insulation on the moisture content was continuous during curing for 28 days, and the moisture content of the samples with the thermal insulation layer was significantly larger.

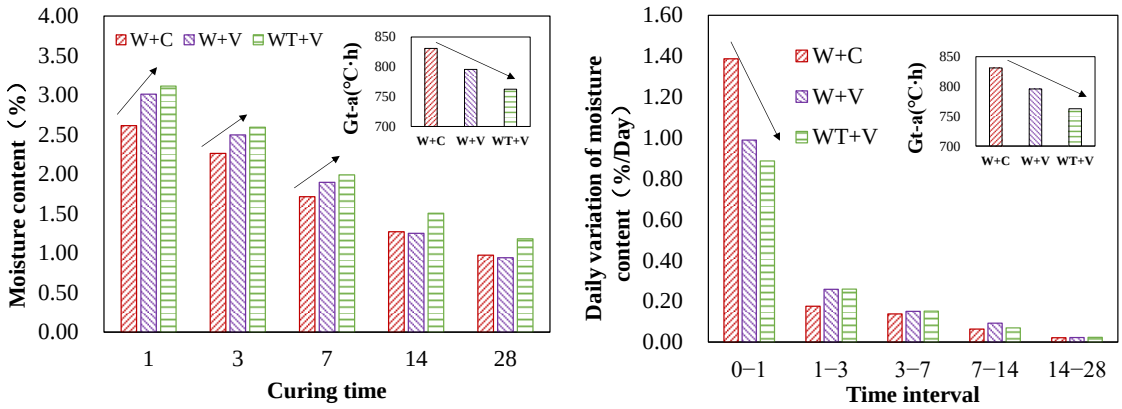

(**a**) Moisture content with Gt-a (**b**) Daily variation of moisture content with Gt-a

Figure 9. Effect of Gt-a on moisture content.

In order to further analyze the influence of the temperature index on the change in moisture content, the daily variation in moisture content was calculated, that is, the difference in moisture content divided by the number of curing days, and the results are shown in Figure 9b. It can be found that the effect of temperature was mainly on the first curing day. The moisture content of W + C decreased 1.4% on the first day, and the variation for W + V was slightly larger than that for WT + V. Subsequently, the daily variation in moisture content of W + C was the smallest among the three methods, which was opposite to its Gt-a. Similarly, the daily variation in moisture content of W + V and WT + V was not the same rank as that of Gt-a except for the first curing day. Therefore, it can be concluded that the effect of different temperature modes on moisture content is mainly reflected in the initial stage of curing, especially the first day.

4.2. Relationship between Moisture Content and Air Void

Figure 10 illustrates the relationship between moisture content and air void during the curing period. A clear linear relationship between moisture content and air void can be observed regardless of the curing method, and the greater the moisture content, the smaller the air void. This indicates that after compaction of the BE-CIR, residual water fills the void, and the free water continues to evaporate, migrate, or be absorbed by cement during curing, resulting in the increase in air void. Meanwhile, there is a maximum value of the air void, which is about 10% when the water content is close to 0%, indicating that if the internal water inside the mixture is completely dissipated, the real air void inside the mixture is about 10%.

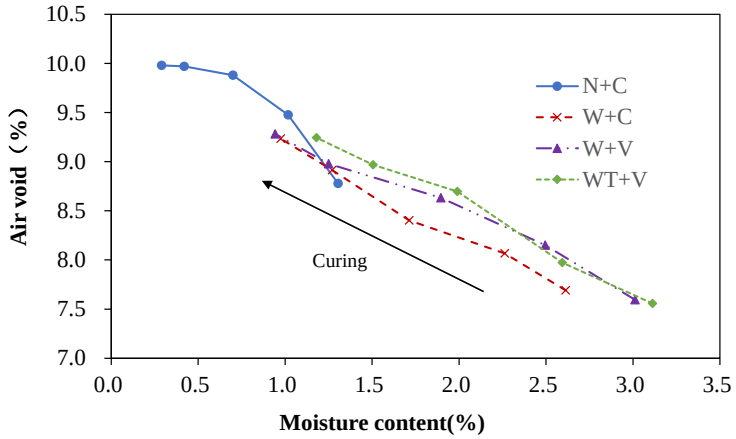

Figure 10. Relationship between moisture content and air void.

4.3. Effect of Moisture Content on ITS

Since there was a certain systematic error in the air void and a strong linear relationship between moisture content and air void, only the effect of moisture content on ITS is analyzed in this section, as shown in Figure 11. From the curve of N + C, it can be found that the relationship between the ITS and moisture content obviously presented two stages. During the first 14 curing days, the moisture content and ITS show a linear relationship, while from 14 to 28 days, ITS increased significantly with only a slight decrease in moisture content. Meanwhile, while the curves of W + C and W + V had similar characteristics, development of ITS with moisture content before and after 14 days of curing was not the same. Therefore, it can be inferred that the strength growth of the BE-CIR during the curing period can be divided into two stages. In the first stage, the growth of ITS is mainly affected by the internal moisture dissipation, high residual water inhibits the hydration of the cement, and prevents the formation of asphalt film. With the continuous loss of moisture during the curing process, the inhibiting effect of water on the hydration of the cement diminishes, leading to a gradual increase in ITS. In the second stage, it can be considered that the free water in the void has basically evaporated. In this stage, more hydration products were formed and better bonded to the bitumen film, resulting in the strength growth of the BE-CIR mixture.

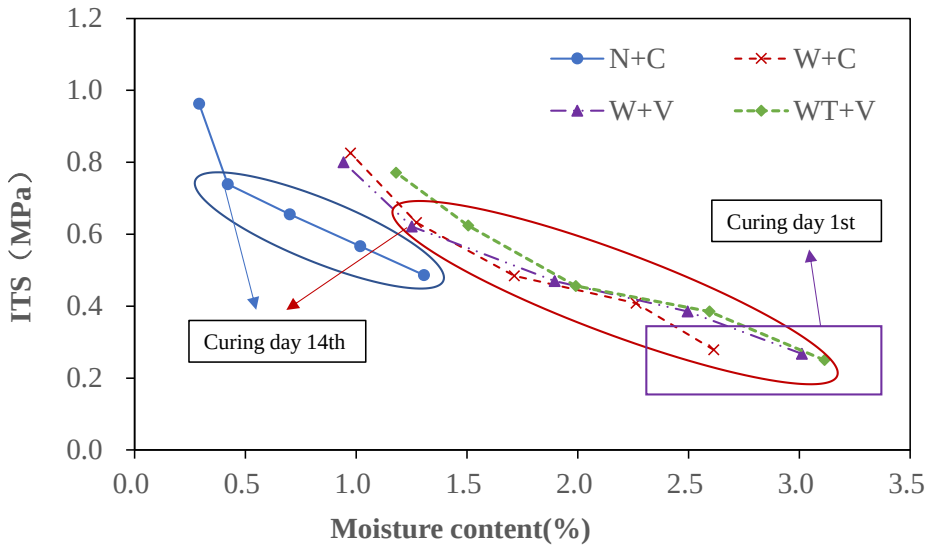

Figure 11. Relationship between moisture content and ITS.

In addition, by comparing the moisture content and ITS of the three curing methods except N + C on the first day of curing, it can be found that the moisture content of the two methods under variable temperature modes is closer. W + C with constant temperature mode had a smaller moisture content, while ITS was basically the same as that of the other two. For the moisture content and ITS after curing for 28 days, the moisture content of WT + V was relatively large and the strength was slightly smaller.

5. Comparison with Field Cores

The field cores were drilled at four curing times, 2, 7, 14, and 28 days, and two samples were taken at each time for testing. Due to the inevitable presence of large amounts of water during the coring process, the moisture content of the field cores could not be tested precisely. Also, this makes it difficult to obtain the actual air void at a special curing time. Therefore, only the ITS of the field cores was tested and the comparison of laboratory samples and field cores is shown in Figure 12. It is also worth noting that the field conditions were more complex than the laboratory conditions, with the temperature and relative humidity varying cyclically every day. The average ambient temperature

during the curing was about 25–30 °C and there were few days of rain. In order to match with the indoor data, the overlay was not constructed during the 28 days of curing in the field-test section.

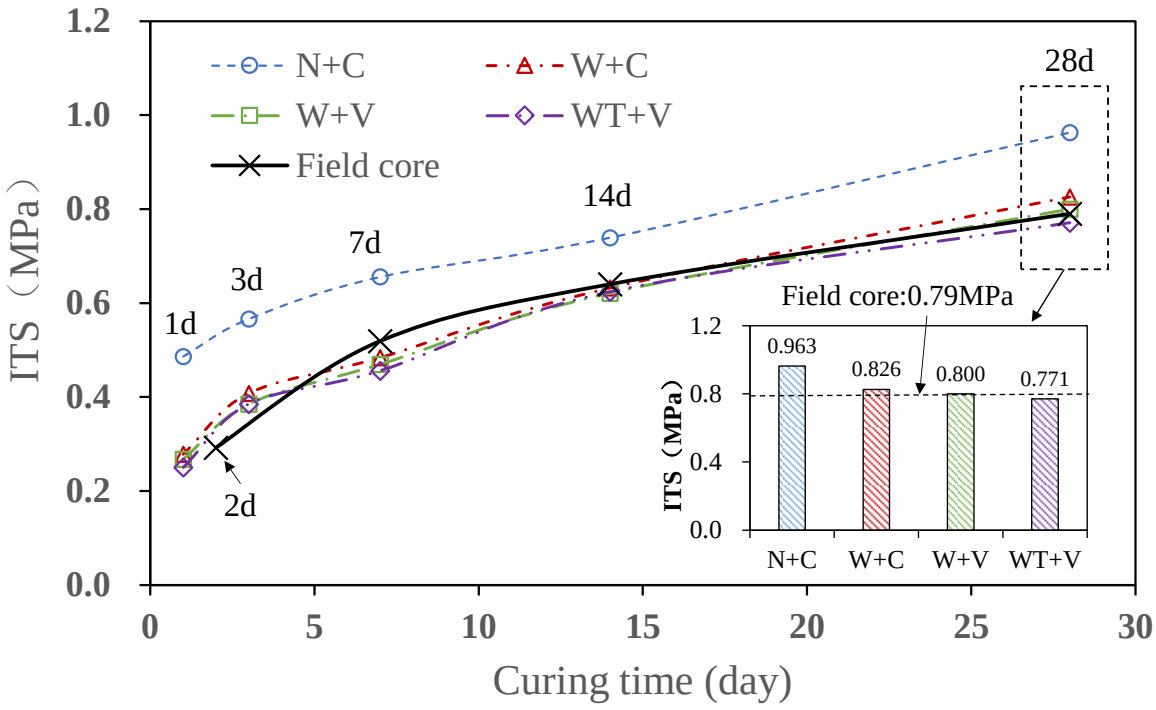

Figure 12. Comparison of ITS between laboratory samples and field cores.

It can be found that the ITS obtained from the curing method of N + C was significantly larger than that of the field cores, indicating that the curing method without any treatment is inconsistent with the actual situation. For the other three curing methods, the increase in ITS over curing time was close to that of the field cores, suggesting that the indoor curing method should consider field-water evaporation. In terms of ITS at a curing time of 28 days, W + V was the closest to the field cores with a difference of only 0.01 MPa, W + C was slightly larger, and WT + V was slightly smaller. Therefore, results of specimens under the curing method of W + V, that is, waterproofing + variable temperature mode, were the closest to those in the actual field curing conditions.

However, considering that the variable temperature mode is relatively complicated and difficult to be realized in the lab, the errors of results between W + C and core samples are also small. The only difference between W + C and W + V is the moisture content in the first few curing days. Therefore, the curing method of W + C, which is the specimen with waterproofing + constant temperature mode, is the most suitable indoor curing method for the BE-CIR, is closer to the real condition, and easier to popularize. To sum up, the indoor curing method for BE-CIR should consider field-water evaporation, while the heat transfer does not have to be considered in the indoor settings.

6. Findings and Conclusions

Four different curing methods considering water evaporation and heat transfer were designed. The variations in temperature indexes, moisture content, air void, and ITS with curing time were tested, and the mutual influence of these indicators was analyzed. Furthermore, results of the laboratory samples after curing for 28 days were compared with the field cores. Several findings and conclusions can be summarized as follows:

(1) The performance development of the BE-CIR mixture cured in the method considering the field-water evaporation condition had significant differences from that with no

treatment (N + C), which was manifested as higher moisture content, lower air void, and ITS under the same curing time. This indicates that the higher water content within the mix may inhibit the hydration of the cement and, thus, lead to a lower strength.

(2) Comparing curing methods considering different heat-transfer conditions, the moisture content showed a rank of W + C < W + V < WT + V, and the ITS had similar regularity. The temperature energy (Gt-a) was better aligned with this ranking than the average temperature. In addition, the differences between the three methods were much smaller than the differences considering water evaporation.

(3) The internal temperature of the mixture was the main factor affecting the variation in moisture content, especially on the first curing day. The air void of the mixture had a strong linear relationship with the moisture content. The relationship between water content and ITS can be divided into two stages. In the first stage, the ITS increased linearly with the decrease in moisture content, indicating that the water dispersion had a significant influence on the strength growth of the BE-CIR mixture. In the second stage, the moisture content decreased slightly and ITS increased rapidly, implying that the free water basically evaporated, and the development of strength was mainly caused by the continuous hydration of cement.

(4) Compared with the results of field cores, N + C had the largest difference in both moisture content and ITS due to the quick water loss rate. The waterproofing and variable temperature mode can better simulate the in situ environmental conditions and delay the water-loss rate of the specimen to a reasonable value.

To sum up, in the laboratory curing setup of BE-CIR, it is important to consider field-water evaporation while the heat-transfer conditions have less influence. Based on this, the waterproofing plus constant temperature mode was considered as the optimal curing method due to its simplicity and a good match. However, at present, only the results of field cores from one actual pavement project were used for the verification of our method. Therefore, more field cores from different sites with different environmental conditions are needed to further verify the adaptability of this curing method.

Although limited in adaptability, the curing method of W + C provides an option to better simulate in situ curing conditions in the laboratory. Different from the purposes of most of the current recommended laboratory curing conditions, the curing method promoted by this paper may not be usually used in the material design of BE-CIR mixtures since it costs more curing time; it is more suitable as a supplementary laboratory test for QC/QA. From the results of this method, pavement engineers and practitioners could achieve a model of mechanical property over curing time to reliably predict the recommended time for the placing of overlay on CIR layers under specific curing conditions.

Author Contributions: Conceptualization, F.N. and Z.C.; Methodology, F.N. and S.X.; Software, Z.Z.; Validation, J.Z.; Formal analysis, Z.Z.; Data curation, Z.Z.; Writing—original draft, Z.Z.; Writing—review & editing, F.N. and J.Z.; Visualization, Z.Z.; Project administration, J.Z.; Funding acquisition, F.N. All authors have read and agreed to the published version of the manuscript.

Funding: This research was funded by the Fundamental Research Funds for the Central Universities (Grant No. 3221002139D) and Shanghai municipal administration commission of housing and urban-rural development (2022-002-002).

Institutional Review Board Statement: Not applicable.

Informed Consent Statement: Not applicable.

Data Availability Statement: The data presented in this study are available on request from the corresponding author.

Conflicts of Interest: The authors declare no conflict of interest.

References

1. Gu, F.; Ma, W.Y.; West, R.C.; Taylor, A.J.; Zhang, Y.Q. Structural performance and sustainability assessment of cold central-plant and in-place recycled asphalt pavements: A case study. *J. Clean. Prod.* **2019**, *208*, 1513–1523. [CrossRef]
2. Modarres, A.; Rahimzadeh, M.; Zarrabi, M. Field investigation of pavement rehabilitation utilizing cold in-place recycling. *Resour. Conserv. Recycl.* **2014**, *83*, 112–120. [CrossRef]
3. Hussein, Z.; Yaacob, H.; Idham, M.; Abdulrahman, S.; Choy, L.; Jaya, R. Rejuvenation of hot mix asphalt incorporating high RAP content: Issues to consider. In *IOP Conference Series: Earth and Environmental Science*; IOP Publishing: Bristol, UK, 2020; p. 012009.
4. Turk, J.; Pranjic, A.M.; Mladenovic, A.; Cotic, Z.; Jurjavcic, P. Environmental comparison of two alternative road pavement rehabilitation techniques: Cold-in-place-recycling versus traditional reconstruction. *J. Clean. Prod.* **2016**, *121*, 45–55. [CrossRef]
5. Alkins, A.E.; Lane, B.; Kazmierowski, T.; Environmental, S.P. Economic, and Social Benefits of In Situ Pavement Recycling. *Transp. Res. Rec.* **2008**, *2084*, 100–103. [CrossRef]
6. Xiao, F.; Yao, S.; Wang, J.; Li, X.; Amirkhanian, S. A literature review on cold recycling technology of asphalt pavement. *Constr. Build. Mater.* **2018**, *180*, 579–604. [CrossRef]
7. Wang, Z.C.; Wang, Q.; Jia, C.X.; Bai, J.R. Thermal evolution of chemical structure and mechanism of oil sands bitumen. *Energy* **2022**, *244*, 123190. [CrossRef]
8. Al-Saffar, Z.H.; Yaacob, H.; Katman, H.Y.; Satar, M.K.I.M.; Bilema, M.; Jaya, R.P.; Eltwati, A.S.; Radeef, H.R.J.S. A review on the durability of recycled asphalt mixtures embraced with rejuvenators. *Sustainability* **2021**, *13*, 8970. [CrossRef]
9. Mohammad, L.N.; Abu-Farsakh, M.Y.; Wu, Z.; Abadie, C. Louisiana experience with foamed recycled asphalt pavement base materials. *Transp. Res. Rec.* **2003**, *1832*, 17–24. [CrossRef]
10. Kuna, K.; Airey, G.; Thom, N. Mix design considerations of foamed bitumen mixtures with reclaimed asphalt pavement material. *Int. J. Pavement Eng.* **2017**, *18*, 902–915. [CrossRef]
11. Konitufe, C.; Abubakar, A.; Baba, A.S.J.C. Influence of Aggregate Size and Shape on the Compressive Strength of Concrete. *Construction* **2023**, *3*, 15–22. [CrossRef]
12. Flores, G.; Gallego, J.; Miranda, L.; Marcobal, J.R. Cold asphalt mix with emulsion and 100% rap: Compaction energy and influence of emulsion and cement content. *Constr. Build. Mater.* **2020**, *250*, 118804. [CrossRef]
13. Deb, P.; Singh, K.L. Mix design, durability and strength enhancement of cold mix asphalt: A state-of-the-art review. *Innov. Infrastruct. Solut.* **2021**, *7*, 61. [CrossRef]
14. Du, S.W. The Optimum Pre-mixing Water Content in Asphalt Emulsion Mixture with Cement. *J. Test. Eval.* **2021**, *49*, 4560–4575. [CrossRef]
15. Lin, J.; Wei, T.; Hong, J.; Zhao, Y.; Liu, J. Research on development mechanism of early-stage strength for cold recycled asphalt mixture using emulsion asphalt. *Constr. Build. Mater.* **2015**, *99*, 137–142. [CrossRef]
16. Golian, M.; Katibeh, H.; Singh, V.P.; Ostad-Ali-Askari, K.; Rostami, H.T. Prediction of tunnelling impact on flow rates of adjacent extraction water wells. *Q. J. Eng. Geol. Hydrogeol.* **2020**, *53*, 236–251. [CrossRef]
17. Yang, Y.H.; Wang, H.B.; Yang, Y.; Zhang, H.Z. Evaluation of the evolution of the structure of cold recycled mixture subjected to wheel tracking using digital image processing. *Constr. Build. Mater.* **2021**, *304*, 124680. [CrossRef]
18. Cardone, F.; Grilli, A.; Bocci, M.; Graziani, A. Curing and temperature sensitivity of cement-bitumen treated materials. *Int. J. Pavement Eng.* **2015**, *16*, 868–880. [CrossRef]
19. Graziani, A.; Godenzoni, C.; Cardone, F.; Bocci, M. Effect of curing on the physical and mechanical properties of cold-recycled bituminous mixtures. *Mater. Des.* **2016**, *95*, 358–369. [CrossRef]
20. Graziani, A.; Iafelice, C.; Raschia, S.; Perraton, D.; Carter, A. A procedure for characterizing the curing process of cold recycled bitumen emulsion mixtures. *Constr. Build. Mater.* **2018**, *173*, 754–762. [CrossRef]
21. Fu, P.C.; Jones, D.; Harvey, J.T.; Halles, F.A. Investigation of the Curing Mechanism of Foamed Asphalt Mixes Based on Micromechanics Principles. *J. Mater. Civ. Eng.* **2010**, *22*, 29–38. [CrossRef]
22. Lee, H.; Im, S. *Examination of Curing Criteria for Cold In-Place Recycling*; Technical Report for Iowa Highway Research Board, University of Iowa: Iowa City, IA, USA, 2008.
23. Pasetto, M.; Pasquini, E.; Baliello, A.; Raschia, S.; Rahmanbeiki, A.; Carter, A.; Perraton, D.; Preti, F.; Gouveia, B.C.S.; Tebaldi, G. Influence of curing on the mechanical properties of cement-bitumen treated materials using foamed bitumen: An interlaboratory test program. In Proceedings of the 9th International Conference on Maintenance and Rehabilitation of Pavements—Mairepav9, Zurich, Switzerland, 1–3 July 2020; Springer: Berlin/Heidelberg, Germany, 2020; pp. 55–65.
24. Kim, Y.; Im, S.; Lee, H.D. Impacts of curing time and moisture content on engineering properties of cold in-place recycling mixtures using foamed or emulsified asphalt. *J. Mater. Civ. Eng.* **2011**, *23*, 542–553. [CrossRef]
25. Tebaldi, G.; Dave, E.V.; Marsac, P.; Muraya, P.; Hugener, M.; Pasetto, M.; Graziani, A.; Grilli, A.; Bocci, M.; Marradi, A.J.R.M.; et al. Synthesis of standards and procedures for specimen preparation and in-field evaluation of cold-recycled asphalt mixtures. *J. Mater. Civ. Eng.* **2014**, *15*, 272–299. [CrossRef]
26. Kuna, K.; Airey, G.; Thom, N.J.C.; Materials, B. Development of a tool to assess in-situ curing of Foamed Bitumen Mixtures. *Constr. Build. Mater.* **2016**, *124*, 55–68. [CrossRef]
27. Yang, W.; Ouyang, J.; Meng, Y.; Han, B.; Sha, Y.J.C.; Materials, B. Effect of curing and compaction on volumetric and mechanical properties of cold-recycled mixture with asphalt emulsion under different cement contents. *Constr. Build. Mater.* **2021**, *297*, 123699. [CrossRef]

28. Ma, X.Y.; Dong, Z.J.; Quan, W.W.; Dong, Y.K.; Tan, Y.Q. Real-time assessment of asphalt pavement moduli and traffic loads using monitoring data from Built-in Sensors: Optimal sensor placement and identification algorithm. *Mech. Syst. Signal Process.* **2023**, *187*, 109930. [CrossRef]
29. Wang, H.; Zhang, X.; Jiang, S.C. A Laboratory and Field Universal Estimation Method for Tire-Pavement Interaction Noise (TPIN) Based on 3D Image Technology. *Sustainability* **2022**, *14*, 12066. [CrossRef]
30. Zhao, Z.L.; Jiang, J.W.; Chen, Z.W.; Ni, F.J. Moisture migration of bitumen emulsion-based cold in-place recycling pavement after compaction: Real-time field measurement and laboratory investigation. *J. Clean. Prod.* **2022**, *360*, 132213. [CrossRef]
31. DOT, J.P. *Applied Manual for Asphalt Emulsion Cold In-Place Recycling Technology*; Department of Transport of Jiangsu province: Nanjing, China, 2010. (In Chinese)
32. *JTG E20-2011*; Standard Test Methods of Bitumen and Bituminous Mixtures for Highway Engineering. Ministry of Transport of the People's Republic of China: Beijing, China, 2011. (In Chinese)
33. *JTG/T 5521-2019*; Technical Specifications for Highway Asphalt Pavement Recycling. Ministry of Transport of the People's Republic of China: Beijing, China, 2019. (In Chinese)
34. *AASHTO T 269*; Standard Method of Test for Percent Air Voids in Compacted Dense and Open Asphalt Mixtures. American Association of State Highway and Transportation Officials: Washington, DC, USA, 2014.